AD-A159 397 SHADOW MOIRE MONITORING OF DAMAGED GRAPHITE/EPOXY SPECIMENS(U) AERONAUTICAL RESEARCH LABS MELBOURNE (AUSTRALIA) K C WATTERS ET AL. FEB 85 ARL-STRUC-TM-398 1/1

UNCLASSIFIED F/G 11/4 NL

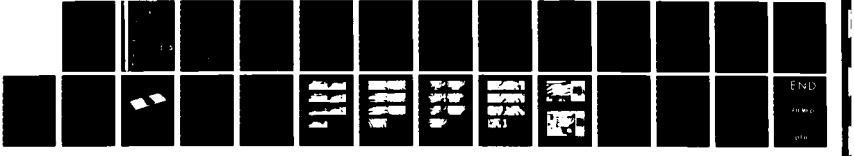

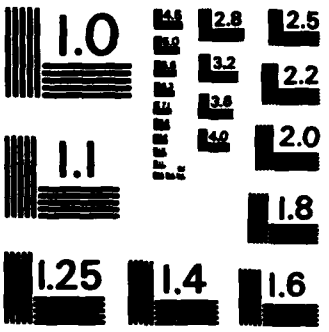

MICROCOPY RESOLUTION TEST CHART
NATIONAL BUREAU OF STANDARDS-1963-A

UNCLASSIFIED

(2)

ARL-SMEC-TM-398

AR-003-991

DEPARTMENT OF DEFENCE

DEFENCE SCIENCE AND TECHNOLOGY ORGANISATION

AERONAUTICAL RESEARCH LABORATORIES

MELBOURNE, VICTORIA

Structures Technical Memorandum 398

ACOUSTIC EMISSION MONITORING OF DAMAGED GRAPHITE/EPOXY SPECIMENS

by

K.C. WATERS, J.G. SPARROW

and R. JONES

COPY No

FEBRUARY 1985

AR-003-991

DEPARTMENT OF DEFENCE

DEFENCE SCIENCE AND TECHNOLOGY ORGANISATION

AERONAUTICAL RESEARCH LABORATORIES

Structures Technical Memorandum 398

SHADOW MOIRE MONITORING OF DAMAGED GRAPHITE/EPOXY SPECIMENS

by

K.C. WATTERS, J.G. SPARROW

and R. JONES

SUMMARY

Compression tests to failure were performed on six graphite/epoxy specimens. Three of the specimens contained an inclusion and the other three had impact damage. During the tests, the out-of-plane deflections of the specimen surfaces were monitored using the shadow moire technique. That technique proved very suitable for the application, and revealed that in the analysis of the inclusion specimens, large deformation theory is required.

POSTAL ADDRESS: Director, Aeronautical Research Laboratories,
P.O. Box 4331, Melbourne, Victoria, 3001, Australia.

CONTENTS

1. INTRODUCTION

Graphite/epoxy composites are prone to a wide range of defects and damage, which can significantly reduce the residual strength. Of the various types of defects, delaminations (i.e. single or multiple internal cracks whose planes are parallel to the surface of the component) arising in service are probably the most insidious, because they cause serious reductions in compression strength and are difficult to detect. In-service delamination damage can occur from a variety of events. The most important source (because the probability of occurrence is high) is impact, i.e. from dropped tools or from stones thrown up from the runway.

It is highly desirable that procedures are available to monitor delamination damage and estimate its severity by analytical means. Indeed, this paper forms part of the work underway at ARL, towards the development of possible methods.

Compression tests to failure were performed on six graphite/epoxy specimens. Three of the specimens contained an inclusion and the other three had impact damage. During the tests, the out-of-plane deflections of the specimen surface were monitored, using the shadow moire technique. Initially, this report describes the performance of the shadow moire technique for this application, in order to generate interest in more widespread use of the technique.*

The results of these tests are then discussed in detail, and it is shown that the inclusion specimens behaved differently from the impacted specimens. ~~It is also shown that~~ in order to analyse the inclusion specimens, large deformation theory must be used.

2. SPECIMENS

The graphite/epoxy material was 2.5 mm and 20 plies thick, according to the specification $(\pm 45/0/90/0)_{2S}$. The specimens were 105 mm long and 45 mm wide, with 40 mm long, 45 mm wide and 1.5 mm thick aluminium grip plates bonded on each end on both sides. This left a working section of 25 mm x 45 mm. A picture of one of the specimens is shown in Figure 1. Specimens 1, 2 and 3 each had a moulded-in 25.4 mm

---

* It is intended that the hardware will be packaged from its current developmental form, so that shadow moire becomes available as a standard measurement technique in Structures Division.

diameter, 0.05 mm thick teflon inclusion between the second and third layers on one side. The centre of the inclusion corresponded approximately with the centre of the working section. Specimens 4, 5 and 6 were each damaged by a 5.4 Joule impact from a 25.4 mm diameter hemispherical-headed piston weighing 1.37 kg, which was dropped down a cylinder from a height of 400 mm. The damage was done to the specimens before the grip plates had been bonded on. The specimens were resting on 25.4 mm thick wooden blocks at their ends and the middle 40 mm long zone was supported on 25.4 mm thick honeycomb. The impact point corresponded approximately with the centre of the working section. A C-scan of the impact damaged specimens showed the damage zone to be roughly circular and approximately 14 mm diameter in each case.

The working section side, which was to be monitored on each specimen, was painted mat white. For the inclusion specimens, this was the surface closest to the inclusion; this was the smooth surface of the graphite/epoxy material. The impact damaged specimens were painted on the opposite side to that which had been impacted, in this case the rough surface of the graphite/epoxy material. The first test on an impact damaged specimen (specimen 4) did not produce any moire fringes. As this was attributed to the surface roughness, the painted surfaces of specimens 5 and 6 were sanded smooth and repainted before testing. This surface preparation proved to be successful.

3. THE SHADOW MOIRE TECHNIQUE

The examination of surface contours by moire patterns is a technique developed many years ago[1], but more recently extended, particularly by Theocaris[2-4]. Moire topography, in which a grating is projected onto the object, which is observed through another grating, has found many applications[5-7]. Alternatively, the projection of a grating onto the surface before and after deformation may be employed[8]. However, the single grating shadow moire technique[9-11] was chosen for the present study.

In the shadow moire procedure, a beam, usually of white light, illuminates the mat-whitened surface of the specimen at an angle α to the specimen and grating normal. A course grating, of pitch P, on glass is positioned parallel, and in close proximity to the mat surface. The shadow of the grating is cast on the mat surface and, together with the reference grating, is viewed by a camera at an angle β to the normal of the grating plane. One of two configurations is generally chosen for single grating shadow moire application. The first of these employs point illumination and point receiving (Figure 2). If the distance separating the camera and light source is D, and they are each at distance L from the grating plane, then geometrical arguments suffice to show that the depth of the out-of-plane displacement of the specimen, corresponding

to the moire pattern, is given by[12]

$$W = \frac{NP}{\tan \alpha + \tan \beta - \frac{NP}{L}} \qquad (1)$$

where N is the fringe order.

The second arrangement uses parallel illumination and parallel receiving. Under these conditions, it can be shown[12] that the equation relating the displacement between the grating plane and the specimen with the moire fringes is

$$W = \frac{NP}{\tan \alpha + \tan \beta} \qquad (2)$$

It is noted that, since generally L >> NP, equations (1) and (2) are close equivalents. In the specific case of viewing normal to the grating plane ($\beta = 0$) both equations reduce to

$$W = \frac{NP}{\tan \alpha} \qquad (3)$$

The above characterisation of the moire fringe pattern has been more strictly developed using communication theory[9] and ray tracing methods[10,13]. Such approaches are required for precise interpretation of high sensitivity measurements, when the observation point and illumination source are at finite distances, but are unnecessary for the pragmatic application of the technique used in this report.

Simple moire fringe observations cannot differentiate the sign of the contours, a hill and a valley appearing identical. A number of solutions to this problem have been developed, among which are the stereo pair method[14], the double exposure two colour method[15], methods based on misalignment, mismatch and grid shifting[16], and various combinations of the above[15]. In the present application, intrinsic knowledge of the deformation shape makes these procedures unnecessary.

4. EXPERIMENTAL ARRANGEMENT

For the tests on the graphite/epoxy specimens, a 100 watt collimated mercury arc light source was used. The angle of illumination was 44° to the grid surface normal. A 240 mm telephoto lens attached to the camera, simulated viewing from infinity. The camera

was approximately 1.1 m from the specimen. Kodak 35 mm Technical Pan film was chosen in order to enhance fringe contrast. In the course of the tests, grids (coarse gratings) of two different frequencies were employed, a fine grid of nominally 20 lines per mm (P = 0.05 mm) and a courser grid of nominally 10 lines per mm (P = 0.1 mm).

A schematic view of the apparatus is shown in Figure 3. The specimens were loaded in a hydraulic mechanical testing machine and only the working section of the specimens was visible between the grips. A long narrow section was cut from a large grid plate, so that it could fit into the 25 mm gap between the grips and be held close to the specimen surface. The painted surface of the specimen faced the grid. Distortion of the surface on the other side of the specimen was not monitored. The grid lines ran vertically, being perpendicular to the long axis of the grid plate. A mat white calibration ramp was glued to one end of the grid plate with a ramp angle of 2.75°. The grid plate was clamped in position in close proximity to the specimen surface, with the specimen and plate coplanar. Clamping was effected at the end opposite to the calibration ramp and there was no mechanical coupling between specimen and plate. The light source, camera and specimen plane was horizontal and perpendicular to the grid lines.

5. PROCEDURE

The grid plate was oriented in front of the specimen surface in such a way as to minimise the fringe pattern at zero load. This was achieved by rotation of the grid plate using clamp adjustments. The gap between the grid plate and the specimen surface was visually adjusted to be about 1-2 mm. This gap was chosen as being just adequate to keep the grid plate clear of the expected surface distortions of the specimen. The tests were performed in daylight conditions.

The specimens were loaded in compression to failure, with photographs of the fringe pattern being taken at regular load increments. For all six specimens the failure of the specimen shattered the glass grid plate. All observers and the testing machine operator were protected from flying glass by protective screens, or helmets with protective visors. Six grid plates were consumed during the course of the tests.

6. RESULTS

The load histories to failure for the six specimens are given in Table 1. The three inclusion specimens failed at about 50 kN, while the three impact damaged specimens failed at about 30 kN.

Moire fringe patterns were obtained successfully for specimens 1, 2, 3, 5 and 6. The surface roughness of specimen 4 broke up the fringe pattern. However, the test on specimen 5 was essentially a repeat of that on specimen 4, and very similar fringe patterns would be expected from the two tests. The fringe patterns from the tests on specimens 1, 3, 5 and 6 are shown in Figures 4, 5, 6 and 7 respectively. Specimen 2 fringes have not been included because they are very similar to those of specimen 1.

The patterns generally take the form of a zone of closed ring fringes superimposed on a background of a linear fringe pattern. The closed ring zone is associated with local out-of-plane buckling or blistering from the impact damage or the inclusion. The size and shape of the outer fringe of this zone is an indicator of the size and shape of the damage zone, and it provides a good monitor of damage growth. The total number of closed ring fringes specifies the maximum out-of-plane deflection of the blister. This will be quantified later.

Although the deflection pattern was minimised at zero load, a background linear fringe pattern developed in the specimens at higher load levels. This effect probably resulted from an overall bending of the specimen, but the exact nature of any such bending was not determined. It may have been caused by misalignment of the end grips since the bottom grip was floating and simply pressed against the machine baseplate, providing the potential for misalignment. Alternatively, a bent shape may have arisen because of some intrinsic specimen asymmetry. This latter possibility is supported by the observation that the background fringe density was higher for the inclusion specimens, as shown by a comparison of the background fringe patterns in Figures 4 and 5 with those in Figures 6 and 7. A specimen with a large inclusion near one surface might be expected to behave asymmetrically.

The fringe contrast in the patterns in Figures 4 and 6 is poor. For these patterns the 20 lines per mm grid was used. The problem is diffraction, whose effect increases with grid frequency and the size of the gap between the grid plate and the specimen surface. It can be seen in Figures 4 and 6 that the centre fringes, where the specimen surface was closest to the grid plate, are in reasonable contrast, but that contrast degenerates from there outward. Following the tests on specimens 1 and 2 (Figure 4) where the fringe contrast was poor, an attempt was made in the test on specimen 5 (Figure 6) to improve contrast by reducing the gap between the grid plate and the specimen surface. Figure 6 shows that this worked at the lower load levels but that, at maximum load, fringe contrast was again dropping off. With the larger deflections of an inclusion specimen, the drop off in contrast would be even greater. It is thus doubtful if the patterns at higher load levels

in Figure 4 could have been improved if the grid plate were initially closer to the specimen surface.

The fringe contrast in the patterns of Figures 5 and 7 is good. For these patterns the 10 lines per mm grid was used.

With the estimated incidence angle of 44°, the sensitivities with the 10 and 20 lines per mm grids have been calculated, using equation 3, as 0.104 and 0.052 mm/fringe respectively. The sensitivities can also be calculated from the fringe patterns on the calibration ramps. These are shown to the right of the specimen fringe patterns in Figures 8 and 9 for the 10 and 20 lines per mm grids respectively. The scale factors shown on Figures 8 and 9 are obtained by relating the specimen widths on those photographs to the known value of 45 mm. The calibration ramp patterns consist of equally spaced vertical fringes and can be characterised by an average fringe spacing, f. From Figures 8 and 9 values of f are 2.17 and 1.11 mm/fringe for the 10 and 20 lines per mm grids respectively. The out-of-plane sensitivities are then found by multiplying these values by the tangent of the ramp angle, 2.75°, the results being 0.104 and 0.053 mm/fringe. These sensitivities are in very close agreement with those calculated from equation 3.

To determine displacements from a moire fringe pattern, it is necessary to assign order numbers to the fringes. Traversing from some zero reference in the pattern, fringes encountered are numbered in ascending order if displacement is increasing from one fringe to the next and descending order if displacement is decreasing. Knowing whether displacement is increasing or decreasing is not always straightforward, and some elaborate methods of fringe ordering are given in references 14-16. Perhaps the simplest method is to use some other displacement transducer to take point readings on the specimen surface, as a guide to fringe ordering. For the application to a blister on the surface of a specimen, fringe ordering presents no problem, since a blister is known to have a simple convex shape with a central maximum. The only difficulty for the fringe patterns in this report is to select a meaningful zero reference amid the background fringe pattern. The procedure adopted was to locate the middle of the blister and move parallel to the linear background fringes until no more fringes were crossed. This was then taken as the zero. The deflection at the middle of the blister was found by counting the number of fringe crossings in a line between it and the zero position. The number was then multiplied by the sensitivity.

The fringes from specimen 1 (Figure 4) show inadequate contrast to allow analysis. However, those from specimens 3, 5 and 6 (Figures 5, 6 and 7) are satisfactory for analysis. The maximum deflections at the middle of the blisters are given in Table 2 for specimens 3, 5 and 6 at a few load levels.

7. DISCUSSION

7.1 Shadow Moire Technique

Diffraction caused the fringes from the 20 lines per mm grid to exhibit poor contrast and, for the inclusion specimens at higher load levels, they became indistinguishable. Contrast could be enhanced by such measures as improving the quality of the grid and eliminating background lighting. However, it is doubtful whether these would be sufficient to render the 20 lines per mm grid suitable for the application described in this report. The 10 lines per mm grid was suitable, and produced distinct fringes of high contrast. Lack of sensitivity is the main limitation of the shadow technique and one would generally wish to use the maximum suitable grid frequency. For the application described in this report, that limit would seem to be somewhere between 10 and 20 lines per mm. This is an area for future investigation.

Several changes can be made to the apparatus to improve the quality of the fringes and to streamline the experimental procedure. Improving the quality of the grid and reducing or eliminating background lighting have been mentioned. The grids used for the tests in this report were produced on glass holographic plates by a photographic reduction process, from a large master grid of frequency 6.6 lines per mm. Limitations of the photographic process and the quality of its lens elements, resulted in the grids not having the same sharp cut-off between the opaque and transparent lines as the master. Grids produced by contact copying higher frequency masters would be of better quality. The experimental procedure would be greatly improved if the grids were clamped to a stand which had fine adjustments for positioning and orienting the grid plate in front of the specimen. Some fiducial marking on the specimen surface would also help to scale and catalogue the photographs.

Calibration of the system from the geometry or from the pattern on the calibration ramp proved equally effective and simple. Perhaps the calibration ramp should be regarded as the primary method, as it gives a permanent record attached to the specimen fringe pattern. Nonetheless, it is recommended that the geometric calibration be performed as a check.

7.2 The Deformation Fields

In recent years an analytical method has been developed for the analysis of delamination damage in composite laminates (17, 18). It is as yet uncertain when it is necessary to use large deformation theory in this analysis. Initially small deformation theory

was used. This approach was not able to fully account for the observed behaviour in the inclusion specimens tested in (18), and (19). However, consulting Table 2 we see that the impact damaged specimens and the inclusion specimens behave very differently. It is clear that the deflection of the inclusion specimens is much larger than the thickness (i.e. 0.25 mm) of the plies above the inclusion. Thus in the analysis of the inclusion specimens large deformation theory is required.

Because the test configuration was not pure compression, although this was the intention, it is not possible to make the same conclusion in the case of the impact damaged specimens. Indeed, given the small thickness of the delamination plies, this slight bending field may have a significant effect on the out-of-plane deflection of the impact damaged laminate.

The experimental results showed that the out-of-plane displacements, over the region of the damage, commenced very early in the tests. Had these tests been in pure compression this would have ruled out the hypothesis that delamination damage is propagated by buckling. A more controlled series of tests is necessary before such a conclusion can be made.

8. CONCLUSION

The shadow moire technique proved very suitable for monitoring out-of-plane deformations in damaged graphite/epoxy specimens. It is envisaged that, in the future, more widespread use of the technique for this application will be made. This simple test has clearly shown that, when analysing inclusion specimens, large deformation theory must be used.

REFERENCES

1. C.A. Sciammarella, The moire method - a review. Proc. Soc. for Exp. Stress Analysis 39, 1982, pp. 418-433.

2. P.S. Theocaris, Moire patterns of isopachics. Journ. Sci. Inst. 41, 1964, pp. 133-138.

3. P.S. Theocaris, Isopachic patterns by the moire method. Exp. Mech. 4, 1964, pp. 153-159

4. P.S. Theocaris, Comments on: Moire topography. Appl. Opt. 10, 1971, p. 1172.

5. P. Benoit, E. Mathieu, J. Horniere, and A. Thomas, Characterization and control of three dimensional objects using fringe projection techniques. Nouvelle Review d'Optique 6, 1975, pp. 65-73.

6. C.A. Miles, and B.S. Speight, Recording the shape of animals by a moire method. J. Phys. E 8, 1975, pp. 773-776.

7. M. Idesawa, T. Yatagai, and T. Soma, Scanning moire method and automatic measurement of 3-D shapes. Appl. Opt. 16, 1977, pp. 2152-2162.

8. J. Der Hovanesian, and Y.Y. Hung, Moire contour-sum contour-difference, and vibration analysis of arbitrary objects. Appl. Opt.10, 1971, pp. 2734-2738.

9. D.M. Meadows, W.O. Johnson, and J.B. Allen, Generation of surface contours by moire patterns. Appl. Opt.9, 1970, pp. 942-947.

10. C. Chiang, Moire patterns from the surface and their application in measuring topography, Brit. J. Appl. Phys. (J. Phys. D),2(2), 1969, pp. 287-292.

11. F.P. Chiang, and C.C. Kin, Some optical techniques of displacement and strain measurements on metal surfaces. Journ. of Metals, 35(5) May 1983, pp. 49-54.

12. F.P. Chiang, Moire methods of strain analysis., in Manual on Experimental Stress Analysis (Ed. A.S. Kobayashi), SESA 1978, Ch. 6, pp. 51-69.

REFERENCES (CONT'D)

13. H. Takasaki, Moire topography. Appl. Opt. 9, 1970, pp. 1467-1472.

14. H. Takasaki, Moire topography. Appl. Opt.12, 1973, pp. 845-850.

15. A. Livnat, O. Kafri, and G. Erez, Hills and valleys analysis in optical mapping and its application to moire contouring. Appl. Opt. 19, 1980, pp. 3396-3400.

16. K. Murakami, and Y. Murakami, A study of the moire topography (An accurate theory and the applicable limit of the divergent light ray method). Bull. of the JSME, 21, 1978, pp. 788-792.

17. A.A. Baker, R. Jones, and R.J. Callinan, Damage tolerance of graphite epoxy composites, J. Composite Structures (in press).

18. R. Jones, W. Broughton, R.F. Mousley, and R.T. Potter, Compression failures of damaged graphite epoxy laminates, J. Composite Structures (in press).

19. R.F. Mousley, In plane compression of damaged laminates, Proc. Structural Impact and Crashworthiness, pp. 494-503, Elsevier Applied Science Publishers, 1984.

TABLE 1 - Load Histories

Specimen Number	Type	Grid Frequency (lines/mm)	Load Sequence of Photos (kN)	Failure Load (no photo) (kN)
1	inclusion	20	0, 10, 20, 0, 10, 20, 30, 40, 45, 50	50
2	inclusion	20	0, 10, 20, 30, 40, 45	47
3	inclusion	10	0, 10, 20, 30, 0, 30, 40, 45, 46	46.5
4	impact	20	0, 10, 20, 25, 28	29.9
5	impact	20	0, 10, 20, 22, 24, 26, 28	29.6
6	impact	10	0, 10, 20, 25, 28, 30, 32	34

TABLE 2 - Maximum Out-of-plane Deflections

Specimen number	Load (kN)	Fringe order of blister middle	Deflection (mm)
3	30	6	0.62
3	45	9	0.94
3	46	10	1.04
5	28	8.25	0.44
6	28	1.75	0.18
6	30	2.5	0.26
6	32	3.25	0.34

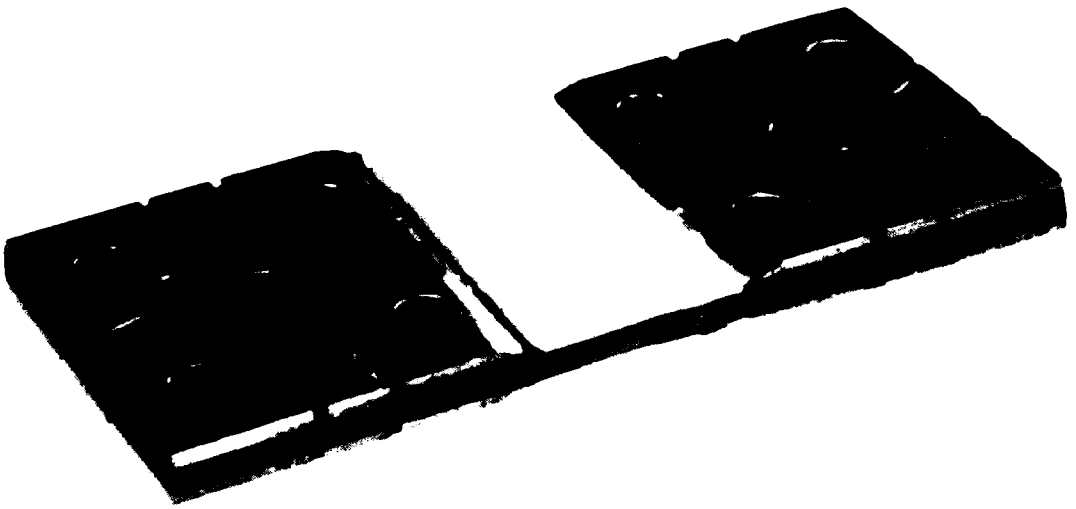

FIG. 1 GRAPHITE/EPOXY SPECIMEN

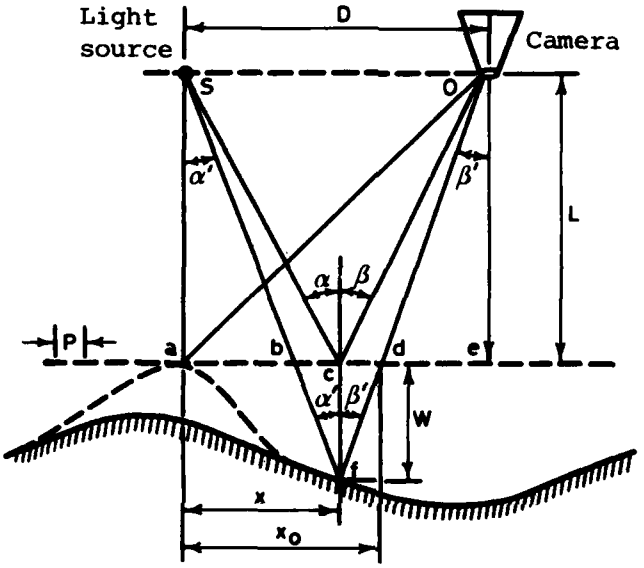

FIG. 2 OPTICAL ARRANGEMENT FOR SHADOW MOIRE MEASUREMENTS WITH POINT ILLUMINATION AND POINT RECEIVING

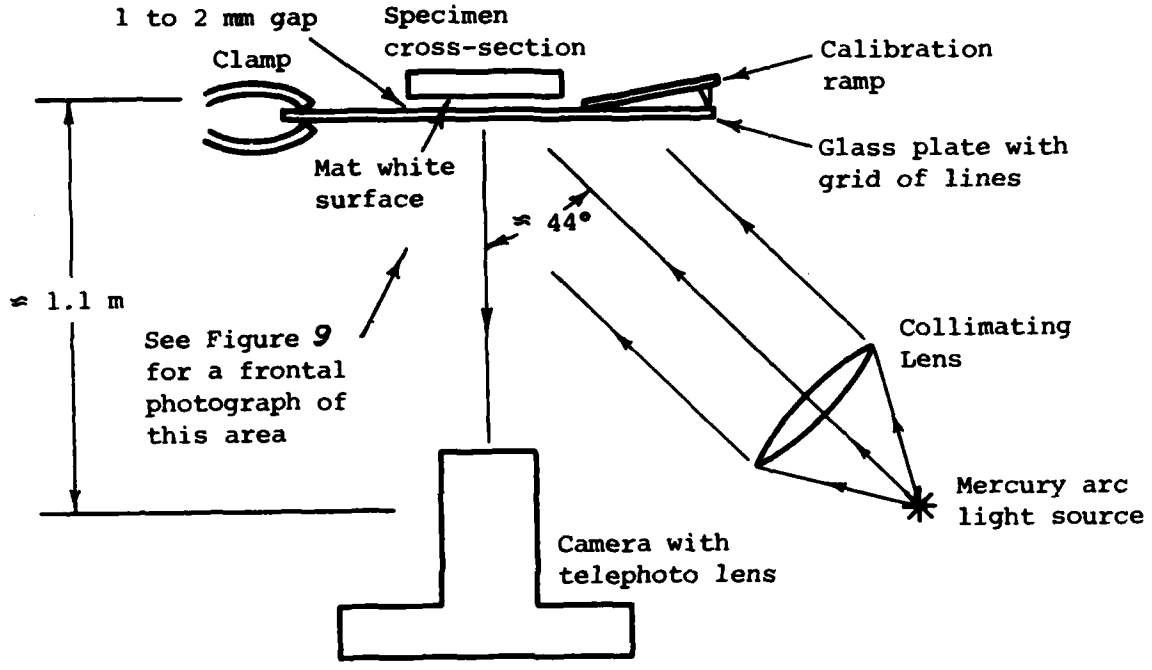

FIG. 3 SHADOW MOIRE APPARATUS - PLAN VIEW

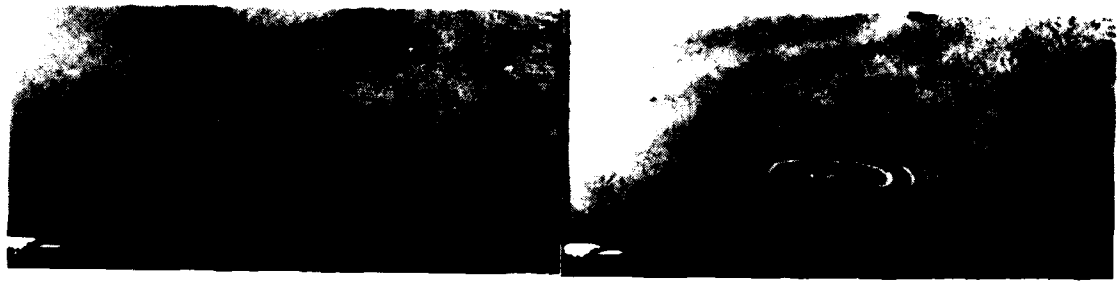

0 kN

40 kN

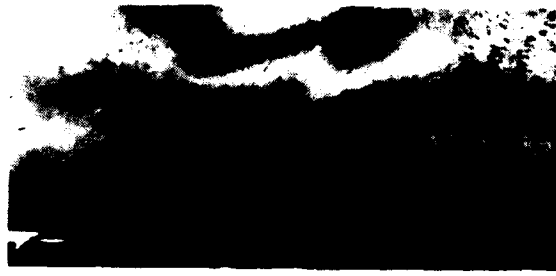

10 kN

45 kN

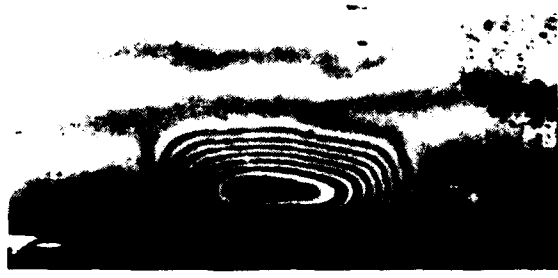

20 kN

50 kN

30 kN

FIG. 4 FRINGE PATTERNS FROM SPECIMEN 1

0 kN 40 kN

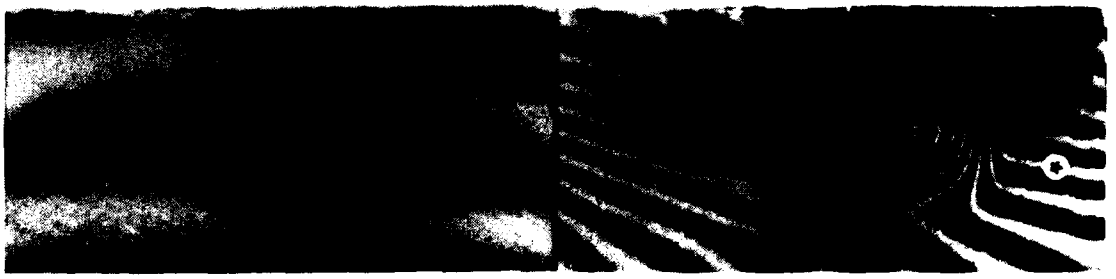

10 kN 45 kN

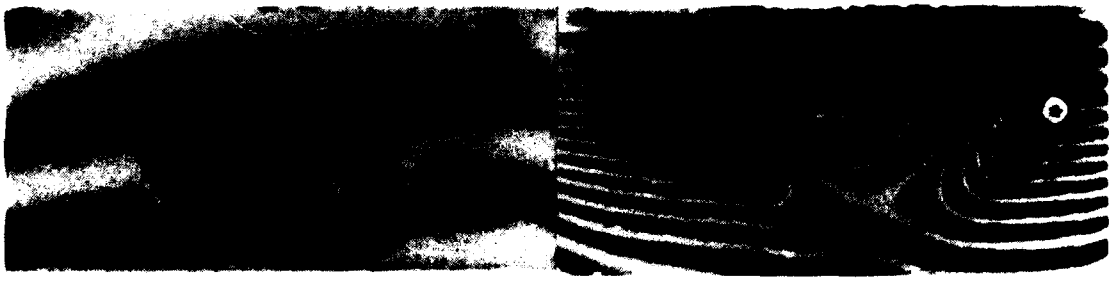

20 kN 46 kN

30 kN

* Zero displacement reference

FIG. 5 FRINGE PATTERNS FROM SPECIMEN 3

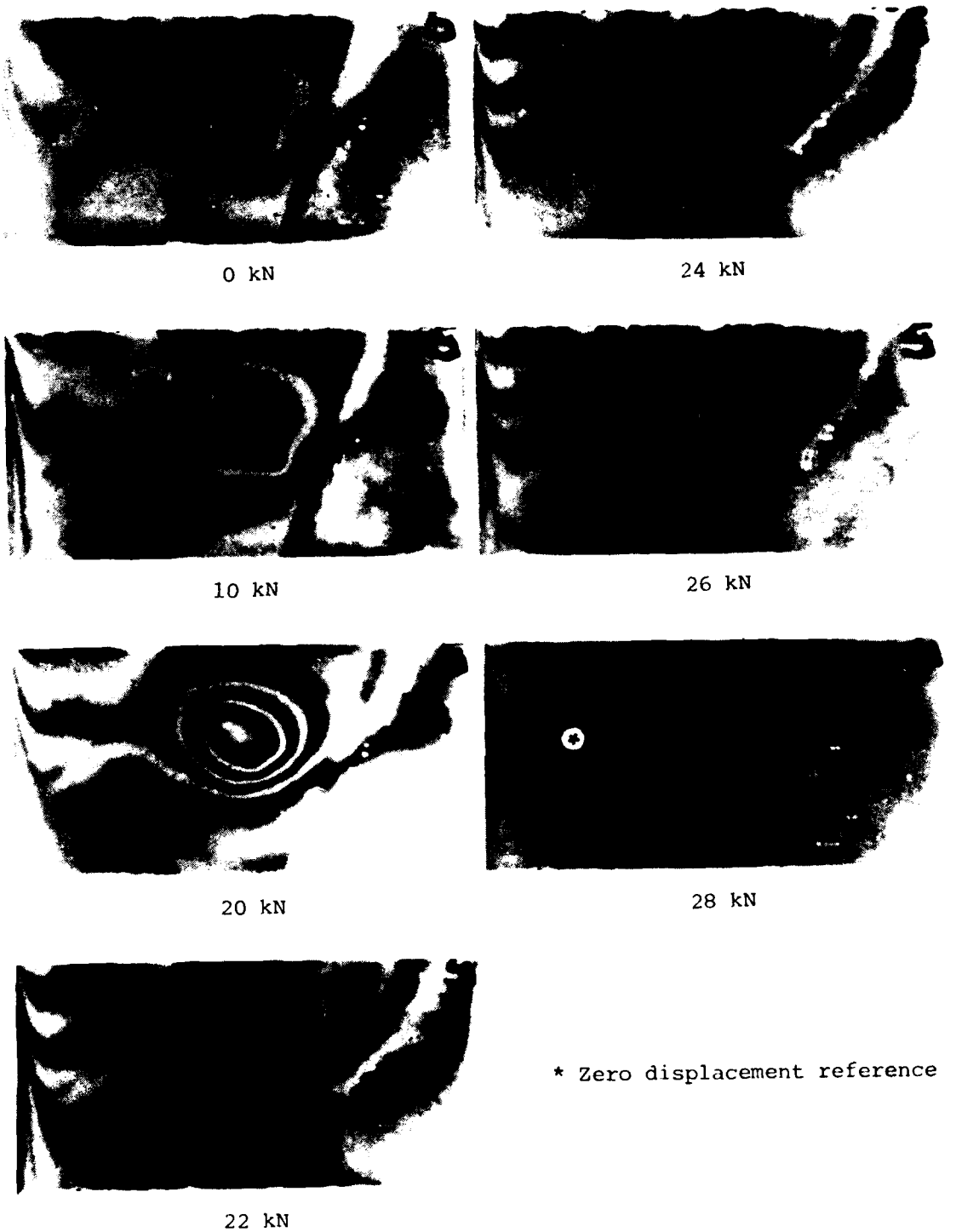

FIG. 6 FRINGE PATTERNS FROM SPECIMEN 5

0 kN 28 kN

10 kN 30 kN

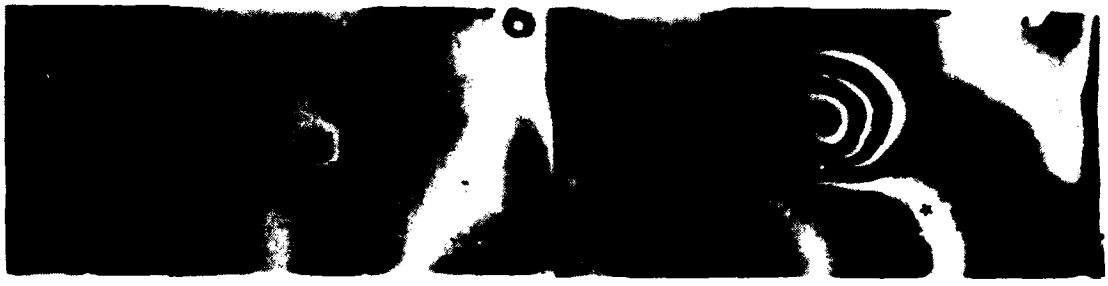

20 kN 32 kN

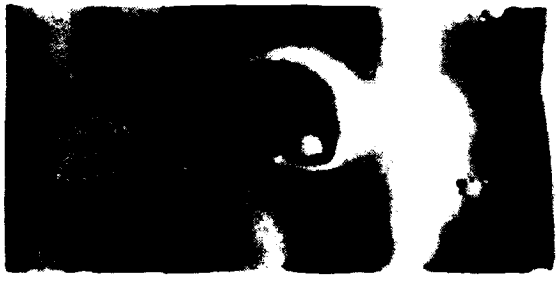

25 kN

* Zero displacement reference

FIG. 7 FRINGE PATTERNS FROM SPECIMEN 6

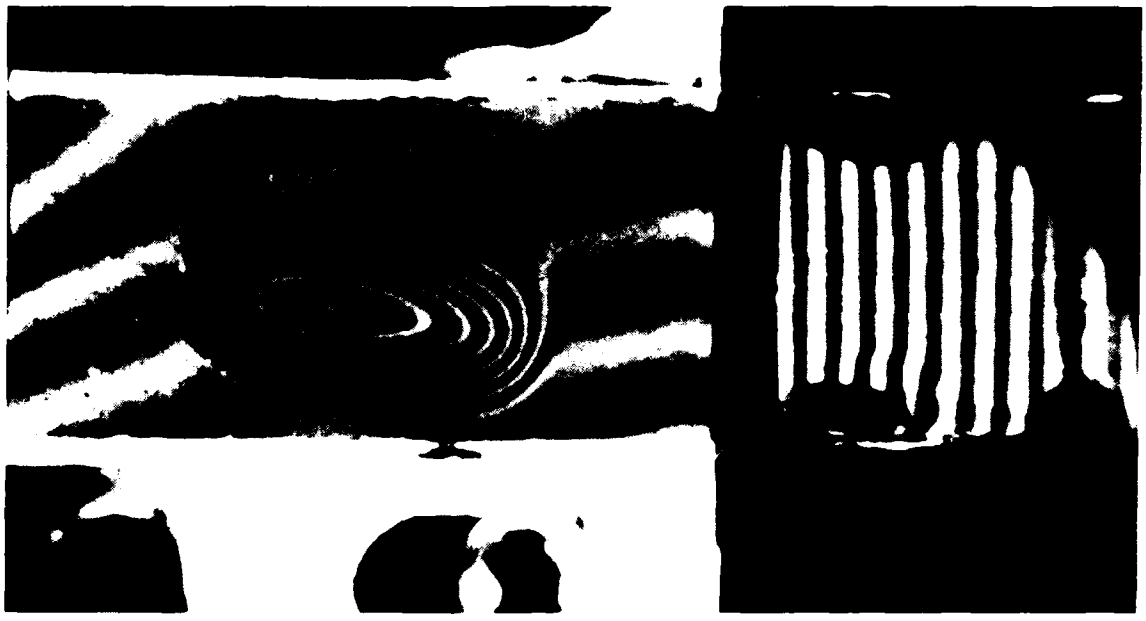

Scale: 1cm = 0.47cm

FIG. 8 SPECIMEN 3, 30KN, 10 1.P.MM GRID

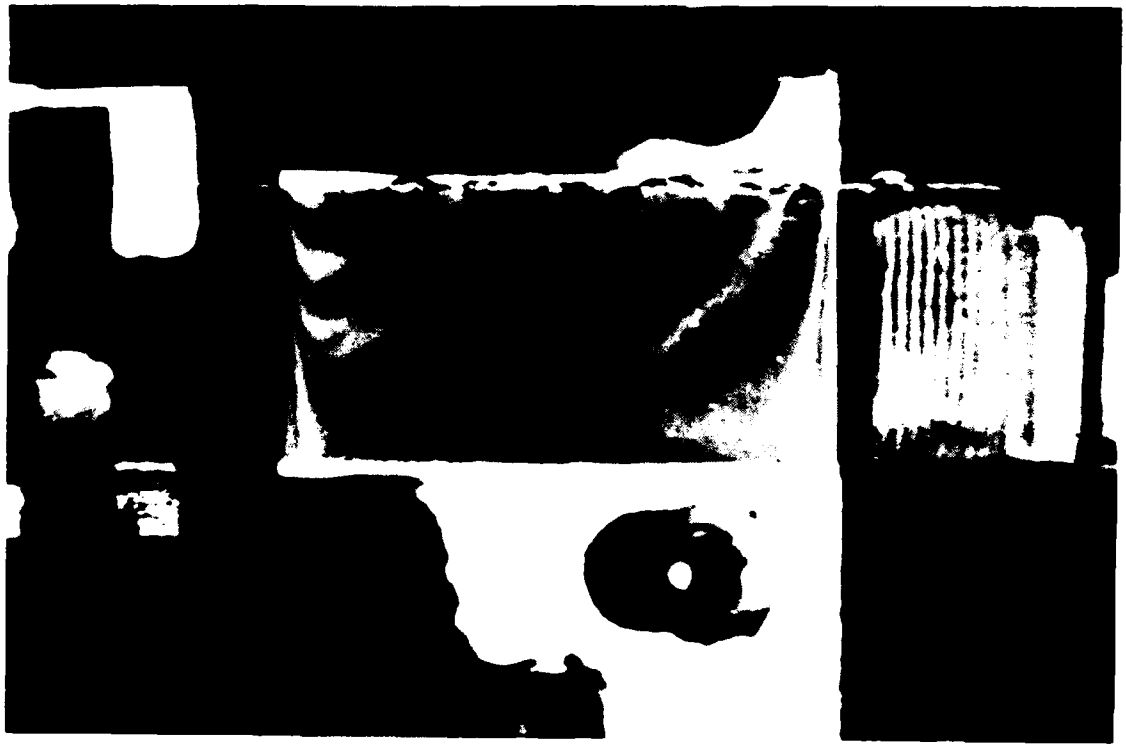

Scale: 1cm = 0.59cm

FIG. 9 SPECIMEN 5, 22KN, 20 1.P.MM GRID

DISTRIBUTION

AUSTRALIA

Department of Defence

Central Office

Chief Defence Scientist)
Deputy Chief Defence Scientist)
Superintendent, Science and Program Administration) 1 copy
Controller, External Relations, Projects and Analytical Studies)
Counsellor, Defence Science (USA) (Doc Data sheet only)
Document Exchange Centre, DISB (18 copies)
Joint Intelligence Organisation
Librarian H Block, Victoria Barracks, Melbourne
Director General - Army Development (NSO) (4 copies)

Aeronautical Research Laboratories

Director
Library
Divisional File - Structures
Authors: K.C. Watters
J.G. Sparrow
R. Jones
A.A. Baker
S.R. Sarrailhe
G. Clark
W. Broughton
R.G. Parker
B. Lawrie

SPARES (10 copies)

TOTAL (47 copies)

A159397

Department of Defence

DOCUMENT CONTROL DATA

1. a. AR No	1. b. Establishment No	2. Document Date	3. Task No
AR-003-991	ARL-STRUC-TM-398	FEBRUARY 1985	DST 83/006

4. Title	5. Security	6. No Pages
SHADOW MOIRE MONITORING OF DAMAGED GRAPHITE/EPOXY SPECIMENS	a. document: UNCLASSIFIED b. title: U c. abstract: U	11 7. No Refs: 19

8. Author(s)	9. Downgrading Instructions
K.C. WATTERS J.G. SPARROW R. JONES	-

10. Corporate Author and Address	11. Authority *(as appropriate)*
Aeronautical Research Laboratories P.O. Box 4331, Melbourne, Vic. 3001	a.Sponsor b.Security c.Downgrading d.Approval

12. Secondary Distribution *(of this document)*

Approved for public release.

Overseas enquirers outside stated limitations should be referred through ASDIS, Defence Information Services Branch, Department of Defence, Campbell Park, CANBERRA ACT 2601

13. a. This document may be ANNOUNCED in catalogues and awareness services available to ...

No limitations

13. b. Citation for other purposes *(ie casual announcement)* may be *(select)* unrestricted *(or)* as for 13 a.

14. Descriptors	15. COSATI Group
Compression test Shadow moire effects Deformation Graphite - epoxy composites	11040 14000

16. Abstract

Compression tests to failure were performed on six graphite/epoxy specimens. Three of the specimens contained an inclusion and the other three had impact damage. During the tests, the out-of-plane deflections of the specimen surfaces were monitored using the shadow moire technique. That technique proved very suitable for the application, and revealed that in the analysis of the inclusion specimens, large deformation theory is required.

This page is to be used to record information which is required by the Establishment for its own use but which will not be added to the DISTIS data base unless specifically requested.

16. Abstract *(Contd)*		
17. Imprint		
Aeronautical Research Laboratories, Melbourne		
18. Document Series and Number	**19. Cost Code**	**20. Type of Report and Period Covered**
Structures Technical Memorandum 398	24 6930	
21. Computer Programs Used		
22. Establishment File Ref(s)		

END

FILMED

10-85

DTIC